Solid-State Chemistry

DOI: 10.1002/anie.201104648

Structural and Electrochemical Diversity in $LiFe_{1-\delta}Zn_{\delta}SO_4F$ Solid Solution: A Fe-Based 3.9 V Positive-Electrode Material**

*Mohammed Ati, Brent C. Melot, Gwenaëlle Rousse, Jean-Noël Chotard, Prabeer Barpanda, and Jean-Marie Tarascon**

Owing to the attractive energy density, high reversibility, and long product lifetime, Li-ion technology has conquered portable electronics[1–3] and now promises to accelerate the integration of environmentally friendly electric vehicles into the marketplace. While the most intensive research efforts started with investigations of oxide-based cathodes, many polyanionic compounds (namely olivine $LiFePO_4$) have emerged as possible cathode systems for sustainable high-volume production.[4] Therefore, in an attempt to increase the energy density of these polyanionic compounds, we have exploited the concept of the inductive effect to enhance the voltage of the battery by replacing PO_4 tetrahedra by SO_4 tetrahedra.

Recently, we discovered a new class of Li-based fluorosulfate materials, among which the tavorite phase of $LiFeSO_4F$ turns out to be an attractive 3.6 V insertion compound.[5] Mindful of the close structural relationship between the precursor and target phases, we have characterized a broad family of fluorosulfates using a robust variety of low-temperature synthetic approaches.[6–9] Practically unknown two years ago, this family ($AMSO_4F$; A = Li or Na, M = Mn, Fe, Co, Ni, or Zn) presently consists of no less than 20 members, many of which present a rich crystal chemistry in combination with interesting electrochemical properties. In addition to the typical $LiFeSO_4F$ tavorite phase we have recently reported the existence of two new polymorphs in this family of compounds: triplite $LiMnSO_4F$[10] and sillimanite $LiZnSO_4F$.[11,12]

[*] M. Ati, B. C. Melot, J.-N. Chotard, Prof. J.-M. Tarascon
Laboratoire de Réactivité et Chimie des Solides
Université de Picardie Jules Verne, CNRS UMR 6007
33, rue Saint Leu, 80039 Amiens (France)
E-mail: jean-marie.tarascon@sc.u-picardie.fr
G. Rousse
Institut de Minéralogie, et de Physique des Milieux Condensés (IMPMC), UMR 7590 CNRS-Université Pierre, et Marie Curie (UPMC) Case courrier 115, 4 Place Jussieu, 75252 Paris Cedex 05 (France)
P. Barpanda
Department of Chemical System Engineering, The University of Tokyo, 5-604, 7-3-1 Hongo, Bunkyo-Ku, 113-8656 Tokyo (Japan)
Prof. J.-M. Tarascon
Collège de France, 11 Place Marcelin Berthelot, 75005 Paris (France)

[**] The authors are thankful to G. Ferey, C. Masquelier, M. Armand, N. Recham for helpful discussions and ALISTORE-ERI for supporting this work. P.B. thanks the Japan Society for the Promotion of Sciences for a JSPS Fellowship at the University of Tokyo.

Supporting information for this article is available on the WWW under http://dx.doi.org/10.1002/anie.201104648.

With respect to electrochemical performances, we found the $LiMnSO_4F$ polymorph to be electrochemically inactive. In contrast, the sillimanite-structured $LiZnSO_4F$ displays a room-temperature conductivity of around 10^{-5} S cm^{-1}, which is close to the current generation of solid-electrolytes, because of the grafting of a layer of ionic liquid to the surface of the particles (see ref. [11]). However, the truly most fascinating aspect of these new polymorphs is that they exist so near the edge of thermodynamic stability when compared to tavorite that small chemical substitutions, on the order of five atomic percent, have been shown to trigger a structural transformation from the tavorite to triplite phase in the $LiFe_{1-\delta}Mn_{\delta}SO_4F$ solid solution.

Motivated by this finding, we expanded our study to see what effect Zn substitution would have on the structure of $LiFeSO_4F$. In a result very similar to the case of Mn, we have found that substitution of Zn causes a transformation from the tavorite to the sillimanite phase (see Figure 1 a). Surprisingly, however, we also encountered a narrow range of composition on the Fe-rich side of the phase diagram, where $LiFe_{1-\delta}Zn_{\delta}SO_4F$ could also be obtained in the triplite structure (see Figure 1 b). More specifically, we found that the product typically consisted of a predominantly single phase with the tavorite–sillimanite transition occurring near $\delta = 0.10$ when made through an ionothermal approach (see Figure 1 c). In contrast, using a traditional solid-state process, we found there is a transition from tavorite to triplite for δ near 0.05 which quickly changes to sillimanite for δ greater than or euqal to 0.15 (see Figure 1 c). For higher Zn content, the sillimanite structure is retained with a linear variation of the unit cell parameters (see Figure S1 in the Supporting Information). We also note that single phase samples could not be obtained using the ceramic approach with δ smaller or equal to 0.05, which seems to indicate a very narrow range of stability for the phase coexistence of the triplite phase within the $LiFe_{1-\delta}Zn_{\delta}SO_4F$ series. Representative values for the unit cell parameters may be found in Table 1.

The crystal structures of tavorite and sillimanite are illustrated in Figure 2. Much like tavorite, the sillimanite structure consists of MO_4F_2 octahedra linked at their corners through F atoms which are oriented in a *trans* configuration with respect to each other giving rise to straight chains which run along the [100] direction of the orthorhombic (*Pnma*) cell of sillimanite. The clearest difference between these structures lays in the orientation of the chains. In triclinic ($P\bar{1}$) tavorite, the chains run along the [001] direction with a rotation from octahedra to octahedra giving a dihedral angle of approximately 27° and are aligned with respect to neighboring chains such that there are wide channels along

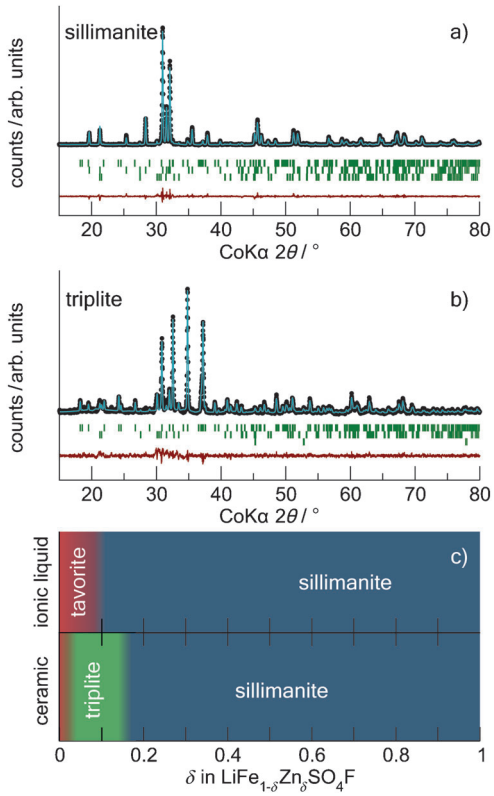

Figure 1. Rietveld refinements of the powder X-ray diffraction patterns collected at room temperature for the a) sillimanite-phase $LiFe_{0.85}Zn_{0.15}SO_4F$ and b) triplite-phase $LiFe_{0.9}Zn_{0.1}SO_4F$. The black dots are experimental points while the blue and red lines are the calculated fit and the difference curve, respectively. c) Phase diagram indicating the structural form adopted depending on the δ value in $LiFe_{1-\delta}Zn_{\delta}SO_4F$. It should be noted that both phases have impurities of residual monohydrate precursor with the triplite phase also containing a small LiF impurity and the sillimanite phase containing a small triplite impurity of approximately 2.4% by mass. Quantification from energy dispersive X-ray (EDX) spectra recorded on numerous particles gave an average composition consistent to ±5 atomic% within the nominal composition. The measurements were repeated in at least five different spots of the samples, and the reported value is an average of these five measurements.

Table 1: Lattice parameters and figures of merit of the Rietveld refinements for $LiFeSO_4F$ in the tavorite phase, $LiFe_{0.9}Zn_{0.1}SO_4F$ in the triplite phase, and $LiFe_{0.85}Zn_{0.15}SO_4F$ in the sillimanite phase. Data for the tavorite phase are taken from ref. [15].

	$LiFeSO_4F$ (tavorite)	$LiFe_{0.9}Zn_{0.1}SO_4F$ (triplite)	$LiFe_{0.85}Zn_{0.15}SO_4F$ (sillimanite)
space group	$P\bar{1}$	$C2/c$	$Pnma$
a [Å]	5.18003 (7)	13.0109 (2)	7.5421 (3)
b [Å]	5.49165 (6)	6.3950 (9)	6.4751 (3)
c [Å]	7.22890 (9)	9.8295 (2)	7.3094 (3)
α [°]	106.4864 (9)	90	90
β [°]	107.186 (9)	119.591 (6)	90
γ [°]	97.9098 (9)	90	90
V/Z [Å^3]	91.397 (4)	88.90 (2)	89.24 (4)
χ^2	2.62	11.7	10.2
R_{Bragg} [%]	2.72	12.4	5.1

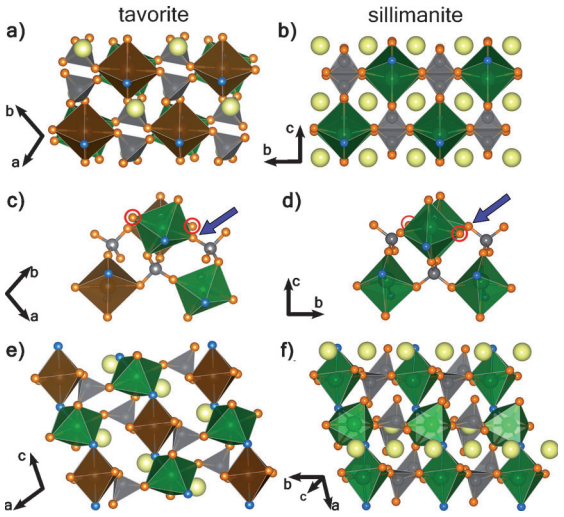

Figure 2. Crystal structure of tavorite (left) and sillimanite (right). The Fe or Zn atoms are located in the middle of the green/brown MO_4F_2 octahedra. The SO_4 tetrahedra are gray, Li atoms are displayed as yellow balls, fluorine atoms are blue, and oxygen atoms are orange. The tavorite structure has channels where lithium ions are located; however, in sillimanite, these channels are partially blocked by the translation of the neighboring chains as indicated by the arrows in (c) and (d).

the [010] direction in which lithium ions are located. In contrast, the octahedra within the chains of sillimanite are in perfect registry down the length of the chain giving no dihedral angle, and one of the neighboring chains which are bridged by the SO_4 tetrahedra is translated by one octahedral unit along the a direction (see Figure 2 c,d). The oxygen atoms circled in red connect to separate chains which are not illustrated. This translation results in a closing of the channels (see Figure 2 e,f), and the creation of new Li sites in sillimanite which are octahedrally coordinated.

The triplite phase is related to sillimanite and tavorite through a disordering of the atomic positions between the transition-metal and Li sites as previously described.[10] Briefly, the triplite structure is composed of two chains of MO_4F_2 highly distorted octahedra (where M is Li or a transition metal and fluorine sits in a *cis* orientation) which share edges and run along the [101] and [010] directions. Comparing the structures, it can be seen that the coordination of Li (Figure 3) evolves from a three-fold environment in tavorite into two highly distorted six-coordinate sites in triplite and finally into more regular octahedra in sillimanite. This change in environment seems to indicate that the site Li occupies in tavorite is less favorable than what is found in triplite and sillimanite. Efforts to determine the relative thermodynamic stability of each phase through calorimetric measurements are presently underway.

The electrochemical properties of the samples in the tavorite (10% Zn), sillimanite (20% Zn), and triplite (10% Zn) phases were tested using Swagelok cells as described in the experimental section. It was found that the sillimanite samples behaved identically to that of the tavorite, therefore the voltage–composition traces are only shown for sillimanite

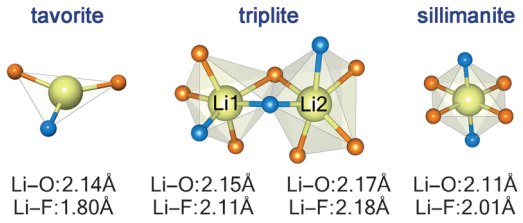

Figure 3. Li coordination environment in the three phases studied. The average Li–O and Li–F distances are given below each panel. In the triplite phase there is an approximately equal distribution of Li between site 1 and site 2.

(Figure 4, upper panel). During the charge to 4.5 V versus Li, 0.68 Li^+ ions are removed from the structure with most (ca. 0.65) being able to be re-inserted on discharge giving reversible capacities ranging from about 100 to 105 mA h g^{-1} with a plateau centered around 3.6 V as deduced from the derivative plot (Figure 4, upper panel inset). This can be compared to the triplite phase which shows a plateau centered near 3.9 V (Figure 4, lower panel) as indicated from both the voltage composition traces and the derivative curve (Figure 4, lower panel inset). The triplite phase has a polarization which is 300 mV larger than that of sillimanite as well as a smaller reversible uptake of Li (0.55 instead of 0.65). Such a result indicates that the Li insertion–deinsertion process is more kinetically limited in the triplite phase.

To understand the changes to the sillimanite structure on delithiation, samples were chemically oxidized using a

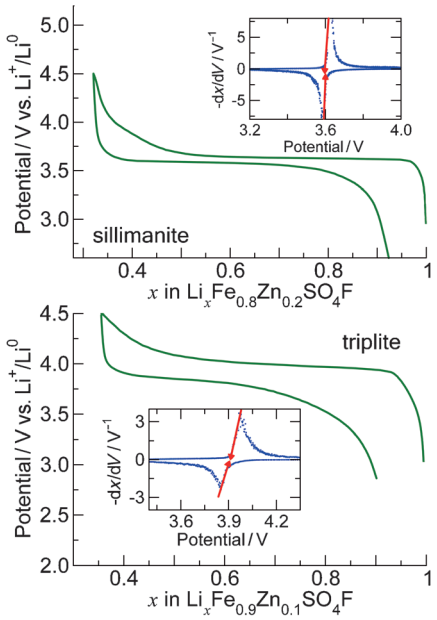

Figure 4. Charge and discharge curves for the sillimanite phase of $Li(Fe_{0.8}Zn_{0.2})SO_4F$ (upper panel) and triplite phase of $Li(Fe_{0.9}Zn_{0.1})SO_4F$ (lower panel) discharged at a C/15 rate. The redox potential observed in the sillimanite phase is found at 3.60 V in close agreement with what is observed for the tavorite phase. In contrast the 3.90 V plateau found in the triplite phase agrees well with what is found for the isostructural $Li(Fe_{0.9}Mn_{0.1})SO_4F$ reported in ref. [10]. The derivative curves ($-dx/dV$) are plotted as a function of the potential V.

mixture of NO_2BF_4 in acetonitrile overnight. The resulting compound could be indexed to an orthorhombic unit cell with lattice parameters of $a = 7.3469(2)$ Å, $b = 6.3394(2)$ Å, $c = 7.2128(2)$ Å with a resulting volume per formula unit of 83.98 $Å^3$ to give a $\Delta V/V = 5.9\,\%$ which is significantly smaller than that of tavorite (10.4 %) but still larger than that of triplite (0.6 %). Interestingly, the redox potential observed for the $LiFe_{1-\delta}Zn_\delta SO_4F$ solid solution is solely dependent upon the structure type regardless of the Zn content (3.9 V for triplite compared to 3.6 V in sillimanite and tavorite). A continuous decrease in the electrode capacity with an increase in the Zn concentration is observed as might be expected considering that Zn is electrochemically inactive.

Overall these results are in good agreement with our results reported for the $LiFe_{1-\delta}Mn_\delta SO_4F$ solid solution[10] where small amounts of Mn were sufficient to induce a tavorite-to-triplite phase transformation and increase the Fe^{2+}/Fe^{3+} redox potential to 3.9 V. More interestingly, however, is that by increasing the Zn content further we are able to access all three phases (tavorite to triplite to sillimanite) with corresponding changes to the redox potential of 3.6 to 3.9 V and back to 3.6 V. Such a result is of great importance in our attempts to better understand the interplay between the structure and electrochemical properties in the various polymorphs of these transition-metal fluorosulfates.

Regarding the synthetic conditions, both approaches (ionic liquid versus ceramic) use the same monohydrate precursor but different reaction environments. In the presence of ionic liquid we find the formation of the tavorite polymorph for small Zn content through a topotactic reaction in which case the ionic liquid appears to control the kinetics of dehydration. In contrast, the ceramic method was found to be strongly affected by the amount of water trapped within the autoclave during the initial heating. The rate of dehydration, which can be controlled by the heating rate, most likely controls a structural change which promotes the growth of either triplite or tavorite. Pinning down the precise structural changes appears essential to ensure our proposed mechanism and therefore in situ high-temperature Mössbauer and NMR experiments are currently underway to clarify this point. Within this context, the fact that both Mn and Zn substitutions promote the transition to triplite may actually result from the mixed-metal precursor, $Fe_{1-\delta}M_\delta SO_4{\cdot}H_2O$, having different kinetics of dehydration compared to the nonsubstituted precursor. Although quite complex, in situ experiments are being designed to monitor this dehydration process.

This potential of 3.9 V is specific to the triplite structure and independent of whether Mn or Zn is substituted. We have tried to rationalize this increased potential on the basis of the ionocovalent character of the metal bonds through a careful analysis of the structural data. The average metal-to-ligand bond lengths are found to be 2.1034, 2.1062, and 2.1508 Å for the sillimanite, tavorite, and triplite phases, respectively. The longest bond corresponds to the greatest ionic character and therefore on this basis it comes as no surprise that the Fe^{2+}/Fe^{3+} redox couple has the highest potential in the triplite phase (3.9 V) and essentially the same value in tavorite and sillimanite phases (3.6 V).

The results which we have presented here set the fluorosulfates apart as a fascinating family of polyanionic compounds because of their rich crystal chemistry and diverse and attractive electrochemistry. Through simple chemical substitution of Zn for Fe, we are able to stabilize three structurally related phases each with distinct electrochemical properties. Improving the kinetics of the 3.9 V electrode, by optimizing the milling time and carbon content, will constitute the next phase of our investigations. Additionally, these phases may therefore be regarded as good candidates to probe the relationship between structure and electrochemical performance; however, their synthesis remains complex with the underlying mechanism being still unclear.

Experimental Section

Synthesis: The solid solution of $LiFe_{1-\delta}Zn_{\delta}SO_4F$ was conducted at low temperature in water-free media using both ionothermal and traditional ceramic preparations. More specifically, stoichiometric amounts of a mixed-metal sulfate monohydrate precursor $(Fe_{1-\delta}Zn_{\delta})SO_4{\cdot}H_2O$, prepared in house from commercial $FeSO_4{\cdot}7H_2O$ and $ZnSO_4{\cdot}H_2O$, as reported earlier,[6] were reacted with LiF either as a mixture of loose powders immersed in an 1-ethyl-3-methylimidazolium-bis(trifluoromethylsulfonyl)imide (EMI-TFSI) ionic liquid (ionothermal process) which was reacted at 275 °C for 2 days or as pressed pellet which was annealed in a sealed Teflon-lined Parr bomb at 260 °C for 5 days.

The purity of all products was analyzed by powder X-ray diffraction (XRD) using a Bruker D8 diffractometer with $Co_{K\alpha}$ radiation ($\lambda_1 = 1.78897$ Å, $\lambda_2 = 1.79285$ Å) equipped with a Vantec detector. All refinements were done using the Rietveld method[14] as implemented in the FullProf suite of programs.[13]

For all electrochemical measurements, standard Swagelok-type cells were assembled using the active materials as the positive electrode and Li metal foil as the negative electrode, separated by two sheets of Whatman GF/D borosilicate glass fibre saturated with 1M $LiPF_6$ solution in 1:1 w/w mixture of ethylene carbonate/dimethyl carbonate as electrolyte. The usual cathode loading was 7 to 10 mg cm^{-2} per cell with active materials consisting of samples which were ball-milled with 35 wt% carbon SP for 18 min. The cells were assembled inside an Ar-filled glove box and were subjected to galvanostatic charge–discharge cycling (at 20 °C) using a Mac-Pile system (Biologic, S.A., Claix, France). The cells were typically cycled between 2.5 and 4.5 V versus Li at 1 Li^+ exchanged per 20 h.

Received: July 5, 2011
Published online: September 16, 2011

Keywords: batteries · electrochemistry · fluorosulfates · lithium · solid-state structures

[1] B. Scrosati, *Nature* **1995**, *373*, 557.
[2] M. Armand, J.-M. Tarascon, *Nature* **2008**, *451*, 652.
[3] M. S. Whittingham, *Chem. Rev.* **2004**, *104*, 4271.
[4] A. K. Padhi, K. S. Nanjundaswamy, J. B. Goodenough, *J. Electrochem. Soc.* **1997**, *144*, 1188.
[5] N. Recham, J.-N. Chotard, L. Dupont, C. Delacourt, W. Walker, M. Armand, J.-M. Tarascon, *Nat. Mater.* **2010**, *9*, 68.
[6] M. Ati, M.-T. Sougrati, N. Recham, P. Barpanda, J. B. Leriche, M. Courty, M. Armand, J.-C. Jumas, J.-M. Tarascon, *J. Electrochem. Soc.* **2010**, *157*, A1007.
[7] M. Ati, W. T. Walker, K. Djellab, M. Armand, N. Recham, J.-M. Tarascon, *J. Electrochem. Solid State Lett.* **2010**, *13*, A150.
[8] M. Ati, L. Dupont, N. Recham, J.-N. Chotard, W. T. Walker, C. Davoisne, P. Barpanda, V. Sarou-Kanian, M. Armand, J.-M. Tarascon, *Chem. Mater.* **2010**, *22*, 4062.
[9] R. Tripathi, T. N. Ramesh, B. L. Ellis, L. F. Nazar, *Angew. Chem.* **2010**, *122*, 8920; *Angew. Chem. Int. Ed.* **2010**, *49*, 8738.
[10] P. Barpanda, M. Ati, B. C. Melot, G. Rousse, J.-N. Chotard, M.-L. Doublet, M. T. Sougrati, S. A. Corr, J. C. Jumas, J.-M. Tarascon, *Nat. Mater.* **2011**, DOI: 10.1038/nmat3093.
[11] P. Barpanda, J.-N. Chotard, N. Recham, C. Delacourt, M. Ati, L. Dupont, M. Armand, J.-M. Tarascon, *Inorg. Chem.* **2010**, *49*, 7401.
[12] P. G. Nagornyi, A. A. Kapshuk, N. V. Stus, N. S. Slobodyanik, A. N. Chernega, *Zh. Neorg. Khim.* **1991**, *36*, 2766.
[13] J. Rodríguez-Carvajal, *Physica B* **1993**, *192*, 55, see http://www.ill.eu/sites/fullprof/.
[14] H. M. Rietveld, *J. Appl. Crystallogr.* **1969**, *2*, 65.
[15] B. C. Melot, G. Rousse, J.-N. Chotard, M. Ati, J. Rodríguez-Carvajal, M. C. Kemei, J.-M. Tarascon, *Chem. Mater.* **2011**, *23*, 2922.

